The Journal of Chemical Physics

Translation-orientation coupling and Cox-Merz rule of liquid hexane

Cite as: J. Chem. Phys. **149**, 204502 (2018); https://doi.org/10.1063/1.5051680
Submitted: 11 August 2018 . Accepted: 13 November 2018 . Published Online: 27 November 2018

Tsuyoshi Yamaguchi, and Tatsuro Matsuoka

View Online Export Citation CrossMark

ARTICLES YOU MAY BE INTERESTED IN

Experimental estimation of the location of liquid-liquid critical point for polyol aqueous solutions
The Journal of Chemical Physics **149**, 204501 (2018); https://doi.org/10.1063/1.5050832

On the geometric dependence of the molecular dipole polarizability in water: A benchmark study of higher-order electron correlation, basis set incompleteness error, core electron effects, and zero-point vibrational contributions
The Journal of Chemical Physics **149**, 204303 (2018); https://doi.org/10.1063/1.5051458

The Stokes-Einstein relation for simple fluids: From hard-sphere to Lennard-Jones via WCA potentials
The Journal of Chemical Physics **149**, 214501 (2018); https://doi.org/10.1063/1.5054577

AIP Publishing

© 2018 Author(s).

Translation-orientation coupling and Cox-Merz rule of liquid hexane

Tsuyoshi Yamaguchi[a] and Tatsuro Matsuoka
Graduate School of Engineering, Nagoya University, Furo-cho B2-3 (611), Chikusa, Nagoya, Aichi 464-8603, Japan

(Received 11 August 2018; accepted 13 November 2018; published online 27 November 2018)

Equilibrium and non-equilibrium molecular dynamics simulations are performed on liquid hexane in order to clarify the origin of the Cox-Merz rule of liquids composed of chain-like molecules. The relation between the frequency-dependent complex shear viscosity and the shear-rate dependent nonlinear viscosity follows the Cox-Merz rule as expected. The slowest viscoelastic relaxation mode is explained by the translation-orientation coupling mechanism, and the saturation of the shear-induced orientational order is observed in the non-equilibrium simulation at the onset of the shear thinning. The origin of the Cox-Merz rule is discussed in terms of the translation-orientation coupling. *Published by AIP Publishing.* https://doi.org/10.1063/1.5051680

I. INTRODUCTION

Shear viscosity is defined as the ratio of shear stress to the applied shear rate. When the applied shear rate is sufficiently small, many fluids exhibit the Newtonian regime of viscosity in which the shear viscosity is independent of the shear rate. However, nonlinear behavior is sometimes observed under strong shear flow, and the description of the nonlinear shear rheology is important in many scientific and engineering fields.[1]

The Cox-Merz rule is one of the empirical rules that describe the nonlinear shear viscosity.[2,3] It states that the shear-rate dependent nonlinear viscosity, $\eta(\dot{\gamma})$, is equal to the amplitude of the frequency-dependent linear complex viscosity, $\eta^*(\omega)$, at $\dot{\gamma} = \omega$, where $\dot{\gamma}$ and ω stand for the shear rate and the angular frequency, respectively. It is well-known empirically that the Cox-Merz rule holds well on polymer systems although its detailed mechanism is still an open question.

We have experimentally investigated the validity of the Cox-Merz rule on three lubrication oils composed of small molecules.[4] The Cox-Merz rule applies to squalene, a chain-like hydrocarbon, while it does not hold on other two oils. We tentatively ascribed the success of the Cox-Merz rule in squalene to its chain-like shape.

Very recently, we studied computationally the shear thinning of the Lennard-Jones (LJ) liquid, which is a representative simple liquid composed of spherical molecules.[5] The slowest viscoelastic relaxation was assigned to the anisotropic shift of the main peak of the structure factor. Due to the narrow width of the main peak, a small amount of the peak shift leads to the deviation of the liquid structure from the equilibrium one, which is the reason for the onset of the shear thinning several times faster than the prediction of the Cox-Merz rule. We consider that the mechanism revealed on the LJ liquid explains the breakdown of the Cox-Merz rule in two lubrication oils.

The next question is the reason why the Cox-Merz rule holds on liquids composed of chain-like molecules. Since polymer is regarded as the elongated limit of the chain-like molecules, this question is of some importance also in polymer physics.

There have been many molecular dynamics (MD) simulation studies on the nonlinear rheology of linear alkanes.[6–13] The shear thinning was reproduced well by non-equilibrium MD simulation. The correspondence between the onset of the shear thinning and the reorientational relaxation time was suggested, and the shear-induced orientational order was also analyzed.

The rank-2 orientational order possesses the same rotational symmetry as the shear stress tensor in liquids composed of anisotropic molecules, and there can be static and dynamic cross correlation between them. The cross correlation between the shear stress and the orientational order is called "translation-orientation coupling."[14–16] There are many experimental methods to analyze the translation-orientation coupling. The first one is the depolarized light scattering, where the coupling is probed through the dynamics of the orientational order.[14,17,18] The second one is the flow birefringence, which measures the collective anisotropy induced by shear flow.[3,19] The ultrasonically induced birefringence can be regarded as the high-frequency version of the flow birefringence.[20,21] The third one is the measurement of the frequency-dependent shear viscosity.[18,21] Due to the translation-orientation coupling, the reorientational relaxation appears in the complex shear viscosity spectrum, and its relaxation amplitude reflects the coupling strength. We have shown in our previous work that the slowest viscoelastic relaxation mode of liquid alkanes is assigned to the translation-orientation coupling.[22]

Given that the reorientational relaxation appears in the frequency-dependent complex shear viscosity, the Cox-Merz rule of liquids composed of chain-like molecules may be

[a]E-mail: yamaguchi.tsuyoshi@material.nagoya-u.ac.jp

ascribed to the translation-orientation coupling when the onset of the shear thinning corresponds to the reorientational relaxation time as was reported in previous studies. The idea is also akin to the stress-optic rule of polymer systems in which nonlinear rheology is related to the nonlinearity of the shear-induced orientation of the bond orientation.[3,23] Therefore, the Cox-Merz rule of liquid alkane is better analyzed in terms of the translation-orientation coupling, which is what we shall undertake in this work.

This paper is composed of five sections. This introductory section, Sec. I, is followed by the theoretical one, Sec. II, which describes the translation-orientation coupling mechanism based on the equilibrium time correlation functions. The conditions of MD simulations are given in Sec. III, and the results are shown in Sec. IV. In Sec. IV, the equilibrium translation-orientation coupling is exhibited first, and the shear thinning is analyzed based on the deviation of the orientational order under shear from the linear response (LR) prediction. The conclusion remarks are given in Sec. V.

II. THEORY

According to the Kubo-Green formula, the frequency-dependent complex shear viscosity, $\eta^*(\omega)$, is given by the Fourier-transformed time correlation function of the shear stress tensor, $\mathbf{P}^{(s)}$, as[24]

$$\eta^*(\omega) = \int_0^\infty e^{-i\omega t} G(t) dt, \tag{1}$$

$$G(t) \equiv \frac{V}{k_B T} \left\langle P_{xy}^{(s)}(0) P_{xy}^{(s)}(t) \right\rangle, \tag{2}$$

where V, k_B, and T stand for the volume of the system, the Boltzmann constant, and the absolute temperature, respectively, and $\langle \ldots \rangle$ means the statistical average under the equilibrium ensemble. The steady state shear viscosity, η_0, is given by the low-frequency limit of $\eta^*(\omega)$ as

$$\eta_0 = \lim_{\omega \to 0} \eta^*(\omega). \tag{3}$$

The collective rank-2 orientational tensor, denoted as $\mathbf{D}$, is usually defined as the sum of the single molecular counterpart as

$$\mathbf{D} \equiv \frac{1}{N} \sum_i \mathbf{D}_i^{(s)}, \tag{4}$$

where $\mathbf{D}^{(s)}{}_i$ indicates the single-molecular rank-2 orientational tensor of molecule i and N stands for the number of molecules in the system. In this work, $\mathbf{D}^{(s)}{}_i$ was defined in terms of the end-to-end vector (the vector between two terminal methyl groups), $\mathbf{r}_{ee,i}$, as

$$\mathbf{D}_i^{(s)} \equiv \frac{\mathbf{r}_{ee,i} \otimes \mathbf{r}_{ee,i}}{|\mathbf{r}_{ee,i}|^2} - \frac{1}{3}\mathbf{1}. \tag{5}$$

The tensor product of two vectors is denoted as $\otimes$ here. It is to be noted here that the discussion in this work does not depend on the details of the definition of the orientational tensor, $\mathbf{D}$.

The collective reorientational dynamics is described by the autocorrelation function of $\mathbf{D}$ as

$$C_R(t) \equiv \frac{N^2 \langle \mathbf{D}(0) : \mathbf{D}(t) \rangle}{\sum_i \left\langle \left| \mathbf{D}_i^{(s)} \right|^2 \right\rangle}, \tag{6}$$

where the colon stands for the scalar product of two tensors. The initial value of $C_R(t)$,

$$g_2 \equiv C_R(0) = \frac{N^2 \left\langle |\mathbf{D}|^2 \right\rangle}{\sum_i \left\langle \left| \mathbf{D}_i^{(s)} \right|^2 \right\rangle}, \tag{7}$$

describes the strength of the static orientational correlation between different molecules.[25] The value of $g_2 = 1$ indicates the absence of the correlation, and the larger value of g_2 means the larger positive correlation. The reorientational relaxation time, τ_R, is defined by the integral of $C_R(t)$ as

$$\tau_R \equiv \frac{1}{C_R(0)} \int_0^\infty C_R(t) dt. \tag{8}$$

The strength of the translation-orientation coupling is described in terms of the translation-orientation coupling constant, denoted as R. The definition of R in terms of time-correlation functions is given by[15]

$$R \equiv \frac{\left| \int_0^\infty \left\langle P_{xy}^{(s)}(0) D_{xy}(t) \right\rangle dt \right|^2}{\int_0^\infty \left\langle P_{xy}^{(s)}(0) P_{xy}^{(s)}(t) \right\rangle dt \int_0^\infty \left\langle D_{xy}(0) D_{xy}(t) \right\rangle dt}. \tag{9}$$

In the diffusive limit, the decay of $C_R(t)$ is proportional to $\exp(-t/\tau_R)$, and the slowest mode of the viscoelastic relaxation is related to the reorientational relaxation through the translation-orientation coupling as

$$\eta^*(\omega) = \eta_0 \left[(1 - R) + \frac{R}{1 + i\omega\tau_R} \right]. \tag{10}$$

The real time version of Eq. (10) is described as

$$\int_0^t G(\tau) d\tau = \eta_0 \left[1 - R e^{-t/\tau_R} \right]. \tag{11}$$

The linear response theory states that the non-equilibrium average under an external field is described in terms of time-correlation functions. The shear-rate dependent nonlinear viscosity, $\eta(\dot\gamma)$, is defined as

$$\eta(\dot\gamma) \equiv -\frac{\left\langle P_{xy}^{(s)} \right\rangle_{\dot\gamma}}{\dot\gamma}, \tag{12}$$

where $\langle \ldots \rangle_{\dot\gamma}$ means the average under the steady simple shear flow in the xy-direction (the direction of the flow velocity is in the x-direction, and its gradient is in the y-direction). The $\dot\gamma \to 0$ limit of $\eta(\dot\gamma)$, η_0, is given by the time correlation function of $P^{(s)}{}_{xy}$ through Eq. (1), which is an example of the linear response theory. The simple shear induces collective orientation in the xy-direction in the linear response regime, and its magnitude is given by

$$\left\langle D_{xy_{\dot\gamma}} \right\rangle = \pm \sqrt{\frac{\eta_0 g_2 \tau_R R}{15 \rho k_B T}} \dot\gamma, \tag{13}$$

where $\rho = N/V$ stands for the number density of the molecules and the sign in the rhs is the same as that of $-\int_0^\infty \left\langle P_{xy}^{(s)}(0) D_{xy}(t) \right\rangle dt$. The derivation of Eq. (13) is described in the Appendix.

It is to be noted here that since R is defined in terms of equilibrium correlation functions, it is applicable solely to systems under weak shear where the linear response theory holds. The nonlinearity in the coupling between the shear stress and the orientational order will be examined numerically in this work using non-equilibrium MD simulation.

The Cox-Merz rule is the empirical relation between the linear viscoelasticity and the nonlinear rheology. When the translation-orientation coupling mechanism is dominant, the former is governed by the relaxation of D_{xy}. It is thus natural to consider that the latter is also determined by the nonlinearity of the response of D_{xy} when the Cox-Merz rule and the translation-orientation coupling mechanism hold. The nonlinearity of $\left\langle D_{xy} \right\rangle_{\dot\gamma}$, which is described as the deviation from Eq. (13), is thus analyzed in this work by means of MD simulation.

III. MD SIMULATION

The equilibrium and non-equilibrium MD simulation runs were performed on liquid hexane composed of 512 molecules. The TraPPE-UA united atom model was employed to describe the intra- and intermolecular interactions of hexane.[26] All the simulation runs were performed under NVT ensemble, and the temperature of the system was controlled to be 298.15 K with the Nosé-Hoover thermostat.[27] The molecules were filled into a cubic cell with the periodic boundary condition. The size of the simulation cell was 4.818 65 nm, which reproduces the density of liquid hexane under the ambient condition.[28] In addition to an equilibrium MD run, the non-equilibrium runs under simple shear were performed with the shear rates of 0.001, 0.003, 0.01, 0.03, 0.1, 0.3, and 1 ps^{-1}. The equation of motion was integrated using the leap-frog algorithm with the time step of 1 fs. For each shear rate, a run of 10 ns was performed first to achieve the equilibrium or steady state, and the subsequent production run of 100 ns length was analyzed. All the sites of hexane are neutral in the TraPPE-UA model, and the intermolecular LJ potential was cut off at 1.4 nm. All the simulation runs were performed using GROMACS 5.1.2 package.[29]

IV. RESULTS AND DISCUSSION

Figure 1 shows the running integral of the equilibrium time correlation function of the shear stress, $G(t)$. After the short-time oscillation, which is ascribed to the intramolecular vibration, the running integral monotonically increases in the ps time regime. The converged value gives $\eta_0 = 0.206$ mPa s, which is consistent with experiments and previous simulation studies.[10,22]

The equilibrium reorientational correlation function, $C_\mathrm{R}(t)$, is shown in Fig. 2. It decays almost exponentially, and it should be noticed that the time scale of the decay is similar to that of $G(t)$ exhibited in Fig. 1. The initial value is $g_2 = C_\mathrm{R}(0) = 1.28$, which suggests the presence of the weak

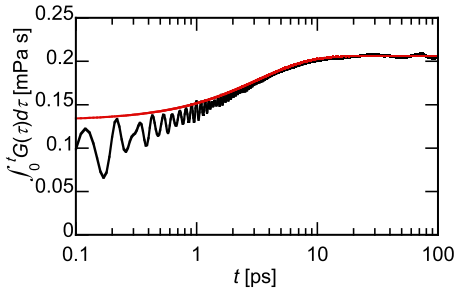

FIG. 1. The running integral of the equilibrium time correlation function of the shear stress, $G(t)$ defined by Eq. (2), is plotted with the black curve and compared with the prediction of the translation-orientation coupling mechanism, Eq. (11) (red curve).

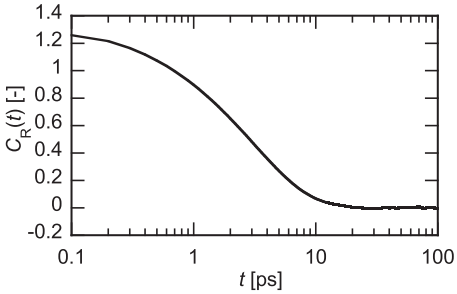

FIG. 2. The equilibrium reorientational correlation function, $C_\mathrm{R}(t)$, defined by Eq. (6).

intermolecular orientational correlation. The integrated reorientational relaxation time, τ_R defined by Eq. (8), is equal to 3.23 ps.

Figure 3 shows the equilibrium cross correlation function between $P^{(s)}{}_{\mathrm{xy}}$ and D_{xy} defined as

$$C_c(t) \equiv \left\langle P_{xy}^{(s)}(0) D_{xy}(t) \right\rangle. \tag{14}$$

The cross correlation function is negative at all the time, indicating that the chains are aligned along the elongation axis under weak shear. The decay rate of $C_\mathrm{c}(t)$ is again close to that of $C_\mathrm{R}(t)$, as is expected from the translation-orientation coupling mechanism. The translation-orientation coupling constant is determined to be $R = 0.36$ from the time integral of $C_\mathrm{c}(t)$ using Eq. (9).

Given the parameters $\eta_0 = 0.206$ mPa s, $\tau_\mathrm{R} = 3.23$ ps, and $R = 0.36$, we can evaluate the running integral of $G(t)$ predicted by the translation-orientation coupling mechanism given by Eq. (11). The result is plotted in Fig. 1 with the red curve and compared with the full-simulation one, black curve.

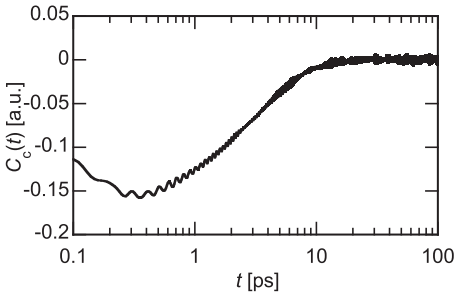

FIG. 3. The equilibrium cross correlation function between the shear stress and the collective orientation.

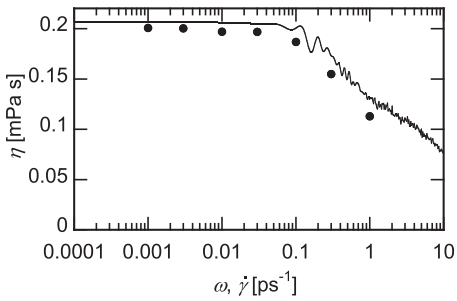

FIG. 4. The amplitude of the linear frequency-dependent complex shear viscosity, $|\eta^*(\omega)|$, is shown with the solid curve and compared with the nonlinear shear-rate dependent viscosity, $\eta(\dot{\gamma})$, plotted with filled circles.

The translation-orientation coupling mechanism describes the slowest mode of the viscoelastic relaxation well.

The time correlation function $G(t)$ is Fourier-transformed to calculate the frequency-dependent shear viscosity, $\eta^*(\omega)$, whose amplitude is shown in Fig. 4 as the solid curve. A viscoelastic relaxation mode is observed at $\omega = 0.3$ ps^{-1}, which corresponds to the reorientational relaxation with $\tau_R = 3.23$ ps. Another relaxation mode is observed at the higher frequency, $\omega \sim 10$ ps^{-1}, which is ascribed to microscopic structural relaxation.

The non-equilibrium shear viscosity, $\eta(\dot{\gamma})$, is independent of the shear rate at the shear rate lower than 0.03 ps^{-1}, which corresponds to the Newtonian regime of the viscosity. Its low-shear limiting value agrees well with the low-frequency limiting value of $\eta^*(\omega)$ as expected. The nonequilibrium shear viscosity exhibits the shear thinning at higher shear rate, that is, the value of $\eta(\dot{\gamma})$ decreases with increasing the shear rate at $\dot{\gamma} > 0.03$ ps^{-1}. The onset shear rate of the shear thinning of $\eta(\dot{\gamma})$ is close to the onset angular frequency of the viscoelasticity of $\eta^*(\omega)$, and these two functions are close to each other at least the shear rate or the angular frequency below 1 ps^{-1}. It can thus be said that Fig. 4 indicates the success of the Cox-Merz rule in liquid hexane.

Since the slowest mode of the linear viscoelastic relaxation is assigned to the orientational relaxation, we consider it natural to analyze the nonlinearity of the response of the orientational order to clarify the origin of the Cox-Merz rule. Figure 5 shows $\langle D_{xy} \rangle_{\dot{\gamma}}$ and $\langle D_{xx} \rangle_{\dot{\gamma}}$ as the functions of the shear rate. The former describes the orientation along the extension axis of the shear deformation, while the latter does that along the flow velocity. The linear-response prediction of the former, Eq. (13), is also plotted together to test the linearity of the orientational response.

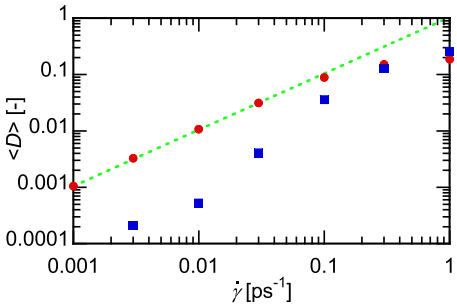

FIG. 5. The average values of D_{xy} (red) and D_{xx} (blue) under shear are plotted against the shear rate. The green dotted line indicates the linear-response prediction of $\langle D_{xy} \rangle_{\dot{\gamma}}$ given by Eq. (13).

The xy-component of the orientational order, $\langle D_{xy} \rangle_{\dot{\gamma}}$, follows the linear response prediction in the Newtonian regime of the shear viscosity, while its increase with the shear rate appears to saturate in the shear-thinning regime. The apparent saturation of the orientational order is thus considered to be related to that of the shear stress. The xx-component is far smaller than the xy-component in the Newtonian regime, while it exceeds at the highest shear rate in this work, 1 ps^{-1}. The alignment along the extension axis thus dominates in the Newtonian regime, and that along the flow direction dominates in the shear-thinning one. The presence of the maximum of $\langle D_{xy} \rangle_{\dot{\gamma}}$ and its decrease under high shear rate were reported by a MD simulation study on model polymers.[30] We expect that the decrease in $\langle D_{xy} \rangle_{\dot{\gamma}}$ with $\dot{\gamma}$ will be also observed in our system at a higher shear rate because the alignment along the flow direction is incompatible with large D_{xy}.

The apparent saturation of $\langle D_{xy} \rangle_{\dot{\gamma}}$ is natural in a sense because it possesses the upper limit of 0.5. The fluctuation of the single-molecule orientational order, defined as $\sqrt{\langle \left| D_{xy}^{(s)} \right|^2 \rangle}$, is equal to $1/\sqrt{15} = 0.258$. Looking at Fig. 5, it is noticed that the deviation of $\langle D_{xy} \rangle_{\dot{\gamma}}$ from the linearity occurs when it becomes close to the spontaneous orientational fluctuation, $\sqrt{\langle \left| D_{xy}^{(s)} \right|^2 \rangle}$, and the shear thinning begins there. In short, the shear-thinning of liquid hexane sets in when the shear-induced orientational order is comparable to the thermal fluctuation of the orientation.

The stress-optic rule for polymeric liquids states that the nonlinearity of the shear stress against the shear rate is described by that of the orientational order if we equate the bond orientation tensor of polymer with the orientational order of whole molecules. Figure 6 shows the correlation between $-\langle P_{xy} \rangle_{\dot{\gamma}}$ and $\langle D_{xy} \rangle_{\dot{\gamma}}$. Their linearity appears to hold at the onset of the shear thinning, $\dot{\gamma} = 0.1$ ps^{-1} and $\langle D_{xy} \rangle_{\dot{\gamma}} \cong 0.1$, and the

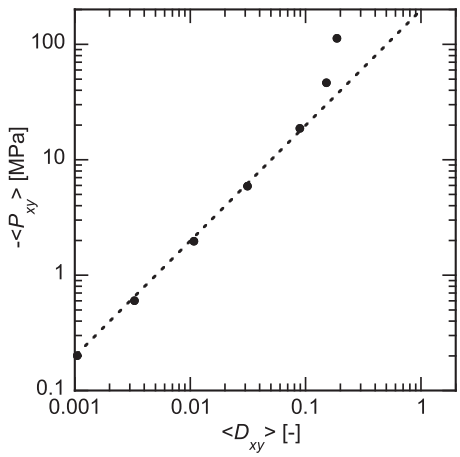

FIG. 6. The average shear stress under shear, $-\langle P_{xy} \rangle_{\dot{\gamma}}$, is correlated with $\langle D_{xy} \rangle_{\dot{\gamma}}$. The results of non-equilibrium MD simulation are plotted with solid circles, while the linear response relation predicted by the equilibrium MD simulation is indicated with the dotted curve.

upward deviation is observed at the higher shear rate. The violation of the stress-optic rule in high shear region was also reported by a MD simulation of polymer liquids.[30]

In Fig. 7, we calculate the distribution of the single-molecule orientation under shear in order to analyze the shear-induced orientational order in detail. Figure 7(a) shows the distribution of $D^{(s)}_{xy}$ at various values of the shear rate. It should be noted here that $P(D^{(s)}_{xy})$ diverges theoretically at $D^{(s)}_{xy} = 0$ in proportional to $\ln(|D^{(s)}_{xy}|)$, while the divergence is not observed in Fig. 7(a) due to the finite width of the sampling grid. As is observed in Fig. 7(a), the equilibrium distribution of $D^{(s)}_{xy}$ is broad, and the deviation of $P(D^{(s)}_{xy})$ from the equilibrium one is small at $\dot{\gamma} \leq 0.01$ ps^{-1} where the shear stress and $\langle D_{xy}\rangle_{\dot{\gamma}}$ behave in linear ways. The deviation then becomes significant in the non-Newtonian regime of the shear viscosity.

The distribution of the xx-component, $D^{(s)}_{xx}$, is shown in Fig. 7(b). In the case of $P(D^{(s)}_{xx})$, its divergence at $-1/3$ is proportional to $1/(D^{(s)}_{xx} + 1/3)$. The deviation of $P(D^{(s)}_{xx})$ from the equilibrium one is small in the low-shear regime, as is expected from small $\langle D_{xx}\rangle_{\dot{\gamma}}$ in Fig. 5. The deviation is not so large even at the shear rate of 0.1 ps^{-1}, which is within the shear-thinning regime, and the strong alignment is observed under the strongly sheared condition, $\dot{\gamma} = 1$ ps^{-1}.

We would like to propose here an idea to understand the shear thinning and the Cox-Merz rule of liquid hexane and the LJ liquid in a unified and consistent way. The slowest mode of the viscoelastic relaxation occurs through the coupling with a microscopic mode of slow dynamics. The microscopic mode is the collective orientation in the case of liquid hexane, and it is the peak shift of the structure factor in the LJ case. In the Newtonian regime of viscosity where weak shear flow is applied, the microscopic mode is distorted linearly as is expected from the linear response theory. With increasing the shear rate, the distortion of the microscopic mode becomes large, and the microscopic liquid structure deviates from the equilibrium one, which leads to the nonlinear response of the shear stress to the shear flow.

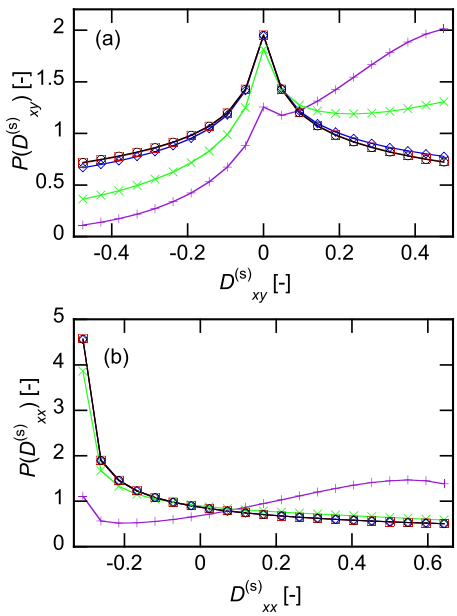

FIG. 7. The distribution of the single-molecule orientational order, (a) $D^{(s)}_{xy}$ and (b) $D^{(s)}_{xx}$, at the shear rates of 0 (equilibrium, black circles), 0.001 ps^{-1} (red squares), 0.01 ps^{-1} (blue diamonds), 0.1 ps^{-1} (green crosses), and 1 ps^{-1} (purple pluses). It should be noted that the divergence of $P(D^{(s)}_{xy})$ at 0 and that of $P(D^{(s)}_{xx})$ at $-1/3$ are suppressed due to the finite widths of the sampling grid. The red curve in panel (a) and the red and the blue curves in panel (b) are difficult to distinguish because they are almost overlapped with the black ones.

The difference between the liquid hexane and the LJ liquid is ascribed to that in the natures of the microscopic modes that are coupled to the slowest viscoelastic relaxation. Since the width of the main peak of the static structure factor is narrow, a small amount of the peak shift leads to the deviation of the liquid structure from the equilibrium one, which explains the stronger shear thinning of the LJ liquid than the prediction of the Cox-Merz rule. On the other hand, the distribution of the orientation is broad as is exhibited in Fig. 7(a), which may explain the wide linear-response regime of the orientational order and the shear stress.

We shall hereafter examine whether the Cox-Merz rule of liquid hexane is elucidated by the idea described above. According to the idea, the shear thinning occurs when the shear-induced orientational order is comparable to the spontaneous orientational fluctuation, which is described as

$$\left\langle D_{xy}\right\rangle_{\dot{\gamma}_0,LR} \cong \sqrt{\left\langle \left|D_{j,xy}\right|^2 \right\rangle} = \frac{1}{\sqrt{15}}. \tag{15}$$

Here, "LR" stands for the linear response. The substitution of Eq. (13) into the left-hand-side of Eq. (15) gives

$$\tau_R \dot{\gamma}_0 \cong \sqrt{\frac{\rho k_B T}{g_2 G_p}}, \tag{16}$$

where $G_\mathrm{p} = \eta_0 R/\tau_\mathrm{R}$ stands for the plateau modulus associated with the slowest mode of the viscoelastic relaxation. According to Eq. (16), the Cox-Merz rule holds when G_p is given by

$$G_p \cong \frac{\rho k_B T}{g_2}. \tag{17}$$

From our equilibrium MD simulation on liquid hexane, the values of G_p, $\rho k_\mathrm{B} T$, and g_2 are 23 MPa, 18.8 MPa, and 1.28, respectively. The condition Eq. (17) thus holds approximately, which explains the Cox-Merz rule in terms of the translation-orientation coupling.

The simple structure of Eq. (17) makes us suspect that there can be a simple logic to derive Eq. (17) for various chain-like liquids in general. We first consider the dependence of G_p on g_2. Although g_2 is usually close to unity in isotropic liquids, it behaves divergently in the isotropic phase of nematogen liquids near the pseudo-critical temperature of the isotropic-nematic transition. As a result, the collective reorientational relaxation time, τ_R, also diverges in proportional to g_2. On the other hand, the temperature dependence of η_0 is rather small, and that of R is also small in the temperature region above 15 K from the pseudo-critical temperature.[17,21] Therefore, the plateau modulus decreases with approaching the pseudo-critical temperature approximately in proportional to $1/\tau_\mathrm{R}$, as is described in Eq. (17).

A possible validation of Eq. (17) may be built on the Stokes-Einstein-Debye (SED) relation, which is a hydrodynamic model on the reorientational relaxation in liquids. The SED relation is given by[17]

$$\tau_R \cong \frac{g_2 V_m \eta_0}{k_B T}, \tag{18}$$

where V_m stands for the hydrodynamic volume of the molecule. The factor g_2 in the numerator converts the single-molecular relaxation time to the collective one.[17,25] The hydrodynamic volume, V_m, is approximated by the van der Waals volume of the molecule as

$$V_m \cong \frac{\xi}{\rho}, \tag{19}$$

where ξ stands for the packing fraction. From Eqs. (18) and (19), G_p is described as

$$G_p = \frac{\eta R}{\tau_R} \cong \frac{\rho k_B T}{g_2} \cdot \frac{R}{\xi}. \tag{20}$$

The typical values of R and ξ of liquids are 0.4 and 0.5, respectively.[15,17,21,22,31] The last factor R/ξ in Eq. (20) is thus close to unity, and Eq. (17) is obtained.

Although the explanation based on the SED relation sounds plausible, it has a weakness in that it is not applicable to polymer systems. The Cox-Merz rule has originally been proposed on polymer systems, and it is well known to hold on these systems although the reason for the Cox-Merz rule is not clarified yet. The slow viscoelastic relaxation of polymer systems is almost exclusively assigned to the coupling with the bond-orientation tensor.[23] The identification of the bond-orientation order of polymer systems with the orientation of the whole molecule in liquids composed of chain-like molecules leads to the idea that the Cox-Merz rule of polymer systems and liquid hexane should be explained in a consistent way. Therefore, we suspect that there must be a more general validation of Eq. (17) based on, for example, the orientational entropy.

Our present analysis suggests that the validity of the Cox-Merz rule strongly depends on the nature of the microscopic dynamic mode that governs the slowest mode of the viscoelastic relaxation. The shift of the narrow peak of the static structure factor breaks the Cox-Merz rule, while the translation-orientation coupling tends to support the Cox-Merz rule. There can be many other microscopic modes that are coupled to slow viscoelastic relaxation. For example, the shift of the charge-alternation mode is important in ionic liquids,[32] and the roles of the prepeak dynamics are suggested on higher alcohols.[22,33] It would thus be interesting to investigate the Cox-Merz rule on these liquids from the view of the microscopic modes of viscoelastic relaxation.

V. CONCLUSION

The frequency-dependent linear complex viscosity and the shear-rate dependent nonlinear viscosity of liquid hexane were calculated by means of equilibrium and non-equilibrium MD simulation, respectively. The comparison between these two quantities indicates that the Cox-Merz rule holds well, which is in harmony with our previous experimental study that the Cox-Merz rule applies to liquids composed of chain-like molecules.

The cross correlation function between the shear stress and the collective orientational order was evaluated based on the translation-orientation coupling mechanism. The slowest mode of the viscoelastic relaxation was described well by the translation-orientation coupling mechanism, which indicates that the slowest viscoelastic relaxation is assigned to the collective reorientational relaxation.

The response of the orientational order to the shear flow was calculated in order to analyze the nonlinear response of the shear stress. The xy-component of the orientational order followed the linear response prediction within the Newtonian regime of shear viscosity, and the saturation of the orientational order was observed in the shear-thinning regime. The deviation of the orientational response from the linear one occurs when the degree of the shear-induced orientation is comparable to the spontaneous fluctuation of the single-molecular orientation. The Cox-Merz rule of liquid hexane was then explained from the view of the translation-orientation coupling mechanism, introducing the SED relation to the orientational plateau modulus.

ACKNOWLEDGMENTS

This work was supported by the Japan Society for the Promotion of Science (JSPS), KAKENHI Grant No. 16K05514.

APPENDIX: DERIVATION OF EQ. (13)

The first factor of the denominator of Eq. (9) is given from Eqs. (1)–(3) as

$$\int_0^\infty \left\langle P_{xy}^{(s)}(0) P_{xy}^{(s)}(t) \right\rangle dt = \frac{k_B T \eta_0}{V}. \tag{A1}$$

The second factor can be calculated from Eqs. (6)–(8) as

$$\int_0^\infty \left\langle D_{xy}(0) D_{xy}(t) \right\rangle dt = \frac{g_2 \tau_R}{15N}. \tag{A2}$$

The substitution of Eqs. (A1) and (A2) into Eq. (9) gives

$$\left| \int_o^\infty \left\langle P_{xy}^{(s)}(0) D_{xy}(t) \right\rangle dt \right|^2 = \frac{k_B T \eta_0 g_2 \tau_R R}{15 \rho V^2}. \tag{A3}$$

The orientational order under steady shear flow is described by the linear response theory as

$$\left\langle D_{xy} \right\rangle_{\dot\gamma} = -\frac{V\dot\gamma}{k_B T} \int_0^\infty \left\langle P_{xy}^{(s)}(0) D_{xy}(t) \right\rangle dt. \tag{A4}$$

The substitution of Eq. (A3) into Eq. (A4) yields

$$\left\langle D_{xy} \right\rangle_{\dot\gamma} = \pm \sqrt{\frac{\eta_0 g_2 \tau_R R}{15 \rho k_B T}}\, \dot\gamma, \tag{A5}$$

where the sign in the rhs is the same as that of $-\int_0^\infty P_{xy}^{(s)}(0) D_{xy}(t) dt$.

[1] R. B. Bird, W. E. Stewart, and E. N. Lightfoot, *Transport Phenomena*, 2nd ed. (John Wiley & Sons, 2007).
[2] W. P. Cox and E. H. Merz, J. Polym. Sci. **28**, 619 (1958).
[3] H. Janeschitz-Kriegl, *Polymer Melt Rheology and Flow Birefringence* (Springer, 1983).

[4]S. Bair, T. Yamaguchi, L. Brouwer, H. Schwarze, P. Vergne, and G. Poll, Tribol. Int. **79**, 126 (2014).
[5]T. Yamaguchi, J. Chem. Phys. **148**, 234507 (2018).
[6]R. Edberg, G. P. Morriss, and D. J. Evans, J. Chem. Phys. **86**, 4555 (1987).
[7]G. P. Morriss, P. J. Daivis, and D. J. Evans, J. Chem. Phys. **94**, 7420 (1991).
[8]P. Padilla and S. Toxvaerd, J. Chem. Phys. **97**, 7687 (1992).
[9]C. J. Mundy, J. I. Siepmann, and M. L. Klein, J. Chem. Phys. **103**, 10192 (1995).
[10]L. I. Kioupis and E. J. Maginn, Chem. Eng. J. **74**, 129 (1999).
[11]N. Mori, T. Tanaka, and K. Nakamura, Nihon Reoroji Gakkaishi **27**, 9 (1999) (in Japanese).
[12]C. McCabe, S. Cui, P. T. Cummings, P. A. Gordon, and R. B. Saeger, J. Chem. Phys. **114**, 1887 (2001).
[13]C. Baig, B. J. Edwards, D. J. Keffer, and H. D. Cochran, J. Chem. Phys. **122**, 184906 (2005).
[14]B. J. Berne and R. Pecora, *Dynamic Light Scattering* (Wiley, 2007).
[15]G. R. Alms, D. R. Bauer, J. I. Brauman, and R. Pecora, J. Chem. Phys. **59**, 5304 (1973).
[16]T. Yamaguchi, M. Hayakawa, T. Matsuoka, and S. Koda, J. Mol. Liq. **147**, 2 (2009).
[17]D. Kivelson and P. A. Madden, Annu. Rev. Phys. Chem. **31**, 523 (1980).
[18]W. Hanai, T. Yamaguchi, and T. Matsuoka, Jpn. J. Appl. Phys., Part 2 **67**, 07LB05 (2018).
[19]D. Kivelson, T. Keyes, and J. Champion, Mol. Phys. **31**, 221 (1976).
[20]T. Matsuoka, J. Miyashita, and S. Koda, Nihon Reoroji Gakkaishi **39**, 43 (2011).
[21]S. Miyake and T. Matsuoka, Jpn. J. Appl. Phys., Part 1 **51**, 07GA10 (2012).
[22]T. Yamaguchi, J. Chem. Phys. **146**, 094511 (2017).
[23]M. Doi and S. F. Edwards, *The Theory of Polymer Dynamics* (Oxford, 1986).
[24]J. P. Hansen and I. R. McDonald, *Theory of Simple Liquids*, 2nd ed. (Academic Press, 1986).
[25]W. G. Rothchild, *Dynamics of Molecular Liquids* (John Wiley & Sons, 1984).
[26]M. G. Martin and J. I. Siepmann, J. Phys. Chem. B **102**, 2569 (1998).
[27]M. P. Allen and D. J. Tildesley, *Computer Simulation of Liquids* (Clarendon Press, Oxford, 1987).
[28]J. A. Riddick, W. B. Bunger, and T. K. Sakano, *Organic Solvents*, 4th ed. (John Wiley & Sons, New York, 1986).
[29]M. J. Abraham, T. Murtola, R. Schulz, S. Pall, J. C. Smith, B. Hess, and E. Lindahl, SoftwareX **1**, 19 (2015).
[30]M. Kröger, W. Loose, and S. Hess, J. Rheol. **37**, 1057 (1993).
[31]J. E. F. Rubio, V. G. Baonza, M. Taravillo, J. Núnez, and M. Cáceres, J. Chem. Phys. **120**, 1426 (2004).
[32]T. Yamaguchi, Phys. Chem. Chem. Phys. **20**, 17809 (2018).
[33]T. Yamaguchi, M. Saito, K. Yoshida, T. Yamaguchi, Y. Yoda, and M. Seto, J. Phys. Chem. Lett. **9**, 298 (2018).